Cavity Ring-Down Laser Absorption Spectroscopy of the $E^3\Delta-X^3\Delta$ Transition of VN

Tongmei Ma, J. W-H. Leung, and A. S-C. Cheung*

Department of Chemistry, The University of Hong Kong, Pokfulam Road, Hong Kong

Received: February 6, 2004; In Final Form: March 15, 2004

The (0,0) band of the electronic transition of VN near 450.5 nm has been investigated using the technique of laser vaporization/reaction with free jet expansion and cavity ring-down laser absorption spectroscopy. A new transition system was observed, which has been assigned as the $E^3\Delta-X^3\Delta$ system. All three $\Delta\Omega = 0$ subband transitions were recorded and rotationally analyzed. A least-squares fit of the measured line positions yielded molecular constants for the new $E^3\Delta$ state. The bond length, r_o, of the $E^3\Delta$ state was determined to be 1.6937 Å, which is the longest among the known states of VN. The $E^3\Delta$ state is expected to arise from the electronic configuration $1\delta^1 10\sigma^1$, where the 10σ orbital is an antibonding orbital. A comparison of the observed electronic states of VN to those of the isoelectronic TiO molecule supports the assignment.

Introduction

Interest in the electronic structure of diatomic molecules containing transition metals has increased in the past decades.[1−6] The importance of these transition metal diatomics ranges from catalysis[7,8] and surface science[9] to astrophysics.[5,6,10] Spectroscopic studies of these diatomic molecules provide important data needed for the understanding of various catalytic processes and chemical bonding in simple metal-containing systems.[3] Transition metal nitrides, in particular, are important in inorganic and biological systems in the industrial fixation of nitrogen.[11] It is well known that transition metal oxide and hydride spectra are observed in the atmosphere of cool M- and S-type stars.[10,12,13] Because of high cosmic abundances of transition elements in stellar objects, it is possible that transition metal nitride molecules may also be found there.

Within the first transition metal period, there has been considerable interest in the spectroscopic properties of vanadium-containing molecules, which include vanadium oxide,[14−19] halides,[20,21] sulfide,[22] and nitride.[23−30] This paper deals with the spectroscopic study of VN. The electronic transitions of VN were first studied by Peter and Dunn[23] and Simard et al.[24] using conventional grating and laser-induced fluorescence spectroscopy (LIFS), respectively. Peter and Dunn[23] recorded the $A^3\Phi-X^3\Delta$ transition and performed rotational analysis of the (0,0) band. Simard et al.[24] reported rotational analysis of the intercombination $d^1\Sigma^+-X^3\Delta_1$ system. Balfour et al.,[25] using a molecular beam source and LIFS, studied the rotational and hyperfine structure of the $D^3\Pi-X^3\Delta$ (0,0) transition and reported accurate rotational and hyperfine constants for both the $D^3\Pi$ and the $X^3\Delta$ states. The permanent electric dipole moments of the $D^3\Pi$ and $X^3\Delta$ states were measured experimentally by Steimle et al.[28] The spectroscopic properties of the low-lying singlet states have recently been studied both theoretically[26] and experimentally.[29,30]

In this paper, we report rotationally resolved spectra of a new electronic transition, namely the $E^3\Delta-X^3\Delta$ system of VN, using the technique of laser vaporization/reaction with supersonic cooling and cavity ring-down laser absorption spectroscopy (CRLAS).[31] The (0,0) band of the $E^3\Delta-X^3\Delta$ transition was recorded and analyzed. Measured line positions were fit to retrieve rotational and spin fine constants for the new $E^3\Delta$ state. In addition, with the use of a molecular orbital energy level diagram, the spectroscopic properties of electronic states arising from various electronic configurations of both the VN and the isoelectronic TiO molecules are compared.

* To whom correspondence should be addressed. Fax: (852) 2857-1586. Tel.: (852) 2859-2155. E-mail: hrsccsc@hku.hk.

Experiment Details

The laser vaporization/reaction free jet expansion apparatus and the cavity ring-down laser absorption experimental setup employed in this work have been described previously.[32] Only a brief description of the experimental conditions is given here. VN molecules were produced by the reaction of laser-vaporized vanadium atoms with ammonia (NH_3). Pulses of 532 nm, 9−10 mJ, and 10 ns from a Nd:YAG laser were focused onto the surface of a vanadium metal rod to generate vanadium atoms. A pulsed valve with appropriate delay released a mixture of 2% NH_3 in helium gas to react with the laser-ablated vanadium atoms. We were also able to produce VN using 0.03% phenyl hydrazine ($C_6H_5NHNH_2$) in helium; however, the signal obtained was generally weaker than those obtained using NH_3. Phenyl hydrazine is a potential nitrogen precursor for use in metal oxide chemical vapor deposition (MOCVD) processes. The operating cycle of the Nd:YAG laser-pulsed valve system was 10 Hz. The backing pressure at the pulsed valve was set to 5 atm. The tunable laser pulses in the visible region were produced by a dye laser pumped by a Nd:YAG laser system.

Two sets of high-reflectance mirrors and two different dyes (Coumarin 460 and Coumarin 503) were necessary to cover the spectral region between 440 and 520 nm. The laser wavelength was calibrated using signals from an optogalvanic cell filled with argon and xenon gases. The dye laser line width was about 0.06 cm^{-1}, and typical pulse energy used in the experiments was 1−3 mJ. The cavity ring-down absorption signal was detected by a photomultiplier tube and fed to a preamplifier before being forwarded to a digital oscilloscope and eventually transferred to a computer for storage. All events for recording the CRLAS signal were coordinated and synchronized by a digital delay generator. It was found that shot-to-shot fluctuation of the cavity ring-down absorption signal was severe, and a steady rotation of the metal rod is necessary to avoid ablating a particular surface for more than a few minutes. Typically, 8−10 laser shots were averaged per data point to maintain an adequate signal-to-noise ratio spectrum. The maximum empty-cavity decay time (1/*e*) for the ring-down

10.1021/jp049441l CCC: $27.50
Published on Web 05/26/2004

TABLE 1: Assigned Rotational Transition Lines of the $E^3\Delta-X^3\Delta$ (0,0) Band of VN (cm^{-1})

J	P_1	Q_1	R_1	P_2	Q_2	R_2	P_3	Q_3	R_3
1		22 194.84	22 196.91						
2	22 192.26	94.44	97.60		22 186.81	22 190.14[a]			
3	90.67	93.90	98.10	22 183.13	86.22	90.67[a]			22 182.70
4	88.81	93.07	98.54[a]	81.35	85.53	91.03[a]		22 177.63	82.98
5	86.81	92.33	98.54[a]	79.38	84.71	91.19[a]	22 171.36	76.73	83.26[a]
6	84.71	91.19	98.54[a]	77.22	83.67	91.19[a]	69.10	75.66	83.26[a]
7	82.44		98.34	74.96	82.44	91.03[a]	66.81	74.39	83.13
8	79.92		97.90	72.46	81.05	90.67[a]	64.28	72.96	82.70
9	77.22		97.31	69.72		90.14[a]	61.62	71.34	82.19
10	74.36		96.53	66.81		89.42	58.72		81.47
11	71.27		95.56	63.89		88.53	55.65		80.60
12	67.93		94.43	60.70		87.48	52.41		79.38
13	64.51		93.07	57.26		86.22	48.92		78.27
14				53.70		84.82	45.32		76.75
15				49.89		83.26	41.59		75.20
16				45.98		81.47	37.63		
17				41.93		79.61	33.55		
18				37.63			29.19		

[a] Blended line.

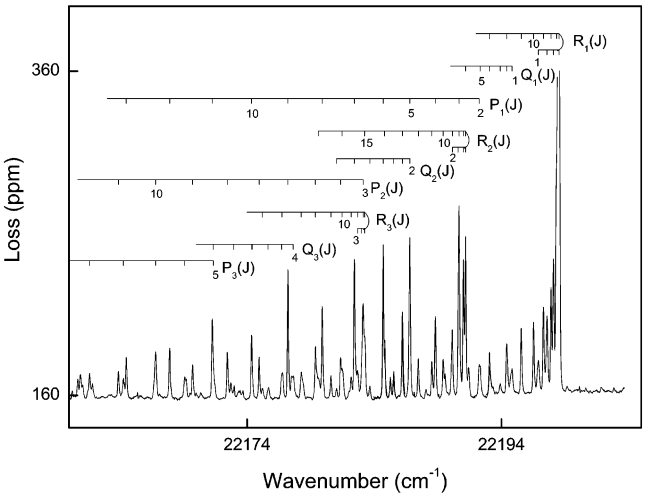

Figure 1. Cavity ring-down laser absorption spectrum of the (0,0) band of the $E^3\Delta-X^3\Delta$ transition of VN.

signal was about 40 μs at 460 nm, corresponding to a loss per pass of about 60 ppm. For the VN spectrum, the highest signal obtained was about 440 ppm. Regular cleaning of the mirrors was necessary to avoid interference arising from the deposition of laser-ablated material. The measured VN lines obtained were calibrated with direct readings from the grating values of the dye laser and converted to vacuum wavelength[33] and then to wavenumbers. The estimated absolute accuracy is about ± 0.2 cm^{-1}; however, the relative accuracy should be better than ± 0.1 cm^{-1}. To obtain information about the vibrational level of the upper state, we also repeated the experiment using $^{15}NH_3$.

Results and Discussion

General Features. The cavity ring-down laser absorption spectrum of VN in the visible region between 440 and 520 nm has been observed and analyzed. The observed band near 450.5 nm shows strong P and R branches, which indicate that the transition is consistent with $\Delta\Lambda = 0$. Detailed rotational analysis confirms that the transition is a $^3\Delta-^3\Delta$ system. By comparison with TiO, a molecule that is isoelectronic with VN, the upper state is probably the fifth triplet excited state, so it is labeled as the $E^3\Delta-X^3\Delta$ transition.

Figure 1 shows the band head region with a resolution of about 0.06 cm^{-1}. It is clearly seen that two subband heads occur at 22 198 and 22 191 cm^{-1}, which correspond to the $E^3\Delta_1-X^3\Delta_1$ and $E^3\Delta_2-X^3\Delta_2$ subband transitions, respectively. The head of the third subband, corresponding to the $E^3\Delta_3-X^3\Delta_3$ transition, is barely noticeable at 22 183 cm^{-1}. Unlike some transition metal diatomic molecules that have been studied, isotopic shifts can be used to confirm the vibrational quantum number of the upper state. VN has no naturally occurring isotope with appreciable abundance. We performed the same experiment again using 2% $^{15}NH_3$ in helium and recorded a portion of the $V^{15}N$ spectrum near the band head region at 22 198 cm^{-1}. A comparison of the R head of the $V^{14}N$ and $V^{15}N$ spectra shows an isotopic shift of less than 0.1 cm^{-1}, which indicates clearly that the transition belongs to the $\Delta v = 0$ sequence. Furthermore, the laser vaporization/reaction free jet expansion source is a low-temperature molecular source, which normally populates the $v = 0$ level of the ground state. Rotational analysis indicated that the lower state B value agrees well with the known B_0 value of the $X^3\Delta$ state. Therefore, the observed band is assigned as the (0,0) band of $E^3\Delta-X^3\Delta$ transition. We searched the wavelength region longer than 450.5 nm and no other VN band was observed, which is consistent with the assignment of the (0,0) band.

Strong R_1 and P_1 branches are readily identified near the band head region. The line assignment was relatively simple because ground-state combination differences, Δ_2F'', can be calculated from published constants.[23] For a $^3\Delta$ (case a)$-^3\Delta$ (case a) transition, the main branches are P_1, Q_1, R_1; P_2, Q_2, R_2; and P_3, Q_3, R_3. We observed all of these main branches. A list of the measured line positions is given in Table 1. Because of relatively large spin$-$orbit separations, the population of the higher spin$-$orbit components, $X^3\Delta_2$ and $X^3\Delta_3$, are low and the transition intensity is generally weak for these subband transitions. For the stronger $E^3\Delta_1-X^3\Delta_1$ subband, the lowest observed J numbers for P_1, Q_1, and R_1 branches are 2, 1, and 1, respectively, which allows the establishment of the component $\Omega'' = \Omega' = 1$ for both states. Close examination of the $Q_1(1)$ and $R_1(1)$ lines shows that the line widths of these two lines are wider than the expected Doppler line width. This is because the $X^3\Delta$ state arises from the electronic configuration involves an unpaired electron in the sσ orbital formed mainly from the vanadium atom 4s orbital, resulting in a large Fermi contact interaction and a large hyperfine splitting.[25] The coupling scheme for the $X^3\Delta$ state conforms to the Hund's case a$_\beta$, and the hyperfine width collapses quickly as J increases.

Determination of Spectroscopic Parameters. The effective molecular Hamiltonian for a $^3\Delta$ state is given[34] by

$$\hat{H}_{\text{eff}} = B\hat{R}^2 - D\hat{R}^4 + A\hat{L}_z\hat{S}_z + \frac{2}{3}\lambda(3\hat{S}_z^2 - \hat{S}^2) + \frac{1}{2}A_D[\hat{L}_z\hat{S}_z, \hat{R}^2]_+ + \frac{1}{3}\lambda_D[3\hat{S}_z^2 - \hat{S}^2, \hat{R}^2]_+ \quad (1)$$

TABLE 2: Molecular Constants for the $X^3\Delta$ and $E^3\Delta$ States of VN (cm^{-1})

parameter	$X^3\Delta$[a]	$E^3\Delta$
T_o	0	22 187.339(9)
B	0.625 328	0.534 999(74)
D	0.91×10^{-6}	0.3×10^{-6} [b]
A	75.503 96	71.44(6)
A_D	−0.025 46	$0.95(5) \times 10^{-4}$
λ	3.369 88	3.08(9)
λ_D	-0.0129×10^{-3}	$-0.0010(7) \times 10^{-3}$
rms	0.05	
$B_{\Omega=1,\mathrm{eff}}$		0.528 24(17)
$B_{\Omega=2,\mathrm{eff}}$		0.536 40(27)
$B_{\Omega=3,\mathrm{eff}}$		0.541 72(39)

[a] Values taken from ref 25. [b] Value fixed in least-squares fit.

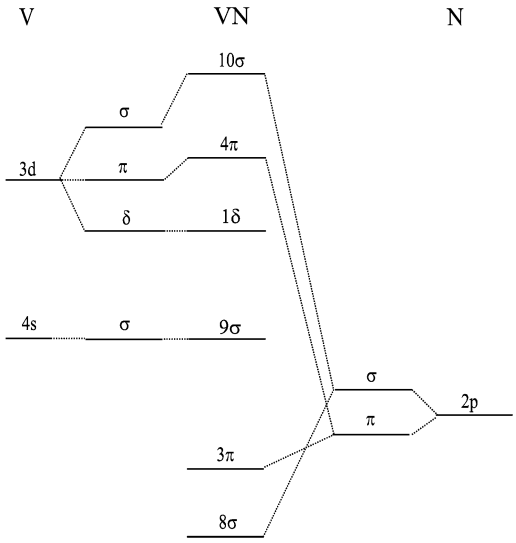

Figure 2. Molecular orbital energy level diagram of VN.

where $[x,y]_+ = xy + yx$ is the anticommutator necessary to preserve the Hermitian form of the Hamiltonian matrix. B and D are respectively the rotational constant and its centrifugal distortion; A and λ are respectively the first-order and second-order spin−orbit parameters; their centrifugal distortion corrections are respectively A_D and λ_D. Matrix elements for the Hamiltonian matrix can be found in papers by Brown et al.[35] and Balfour et al.[25] Least-squares fitting of the observed line positions were performed in two stages. First, the P, Q, and R branches of each subband were fit individually to obtain the effective rotational constant, $B_{\Omega,\mathrm{eff}}$, and the subband origin. Subsequently, all the transition line positions were merged together and fit to a Hamiltonian matrix for the $^3\Delta$ state for both excited and ground states. Since Balfour et al.[25] obtained accurate molecular constants for the $v = 0$ level of the $X^3\Delta$ state, their values were used and held fixed in the fit. The root-mean-square error of the final fit was 0.05 cm^{-1}. Molecular constants obtained are listed in Table 2. The experimentally determined bond length, r_o, for the $E^3\Delta$ state is 1.6937 Å.

Electronic Configurations. Ab initio calculations performed by Harrison[26] indicate that the energy order of excited electronic states of VN is very similar to that of the isoelectronic TiO molecule.[36−38] Figure 2 shows a molecular orbital (MO) energy level diagram of VN formed from the vanadium 4s and 3d atomic orbitals (AOs) and the nitrogen 2p AOs. The lower energy 8σ and 3π MOs and the higher energy antibonding 10σ and 4π MOs are formed from the nitrogen 2p AO and vanadium 3dσ, 3dπ, 4pσ, and 4pπ AOs. The 9σ MO is essentially a vanadium 4s AO. The 1δ MO is almost a pure vanadium 3dδ AO because there is no other orbital of δ symmetry lying nearby.

TABLE 3: Spectroscopic Constants for Low-Lying Triplet and Singlet States of TiO and VN (cm^{-1})

elect config	state	TiO	state	VN
$9\sigma^1 1\delta_1$	$X^3\Delta$	$B_e = 0.534\,51$ $r_e = 1.6202$[a] $A = 50.65$	$X^3\Delta$	$B_o = 0.625\,328$ $r_o = 1.5666$[a] $A = 75.503$
$9\sigma^1 4\pi^1$	$E^3\Pi$	$T_o = 11\,925.03$ $B_o = 0.5155$ $r_\sigma = 1.6512$ $A = 86.86$		
$1\delta^2$	$D^3\Sigma^-$	$T_o = 12\,284$		
$1\delta^1 4\pi^1$	$A^3\Phi$	$T_o = 14\,094.173$ $B_o = 0.505\,69$ $r_o = 1.6671$ $A = 57.3668$	$A^3\Phi$	$T_o = 14\,313.247$ $B_o = 0.610\,85$ $r_o = 1.5851$ $A = 78$
$1\delta^1 4\pi^1$	$B^3\Pi$	$T_o = 16\,147$ $B_o = 0.506\,174$ $r_o = 1.6663$ $A = 20.81$	$D^3\Pi$	$T_o = 16\,026.191$ $B_o = 0.609\,145$ $r_o = 1.5872$ $A = 54.567$
$1\delta^1 10\sigma^1$	$C^3\Delta$	$T_o = 19\,339.73$ $B_o = 0.489\,88$ $r_o = 1.6938$ $A = 46.1$	$E^3\Delta$	$T_o = 22\,187.339$ $B_o = 0.534\,99$ $r_o = 1.6937$ $A = 71.43$
$9\sigma^1 1\delta^1$	$a^1\Delta$	$T_o = 3444.367$ $B_o = 0.536\,287$ r_o(Å) = 1.6189	$a^1\Delta$	$T_o = a$ $B_o = 0.634\,792$ r_o(Å) = 1.5549
$9\sigma^2$	$d^1\Sigma^+$	$T_o = 5663$ $B_o = 0.547\,702$ $r_o = 1.6019$	$b^1\Sigma^+$	$T_o = 10\,952.69$ $B_o = 0.617\,896$ $r_o = 1.5760$
$9\sigma^1 4\pi^1$	$b^1\Pi$	$T_o = 14\,717.185$ $B_o = 0.511\,99$ $r_o = 1.6568$		
$1\delta^2$			$d^1\Sigma^+$	$T_o = 16\,220.187$ $B_e = 0.62\,861$ $r_e = 1.5625$
$1\delta^1 4\pi^1$			$e^1\Pi$	$T_o = a + 14\,292.76$ $B_o = 0.619\,123$ $r_o = 1.5744$
$1\delta^1 4\pi^1$	$c^1\Phi$	$T_o = 21\,284.957$ $B_o = 0.521\,366$ $r_o = 1.6419$	$f^1\Phi$	$T_o = a + 17\,432.31$ $B_o = 0.616\,718$ $r_o = 1.57754$
$1\delta^1 10\sigma^1$	$f^1\Delta$	$T_o = 22\,513.355$ $B_o = 0.502\,363$ $r_o = 1.6726$		
$9\sigma^1 10\sigma^1$	$e^1\Sigma^+$	$T_o = 29\,960.592$ $B_o = 0.488\,25$ $r_o = 1.6966$		

[a] r_e and r_o are in Å unit.

The observed electronic states can easily be understood from this molecular orbital diagram. We compare the spectroscopic properties of electronic states of VN with those of the isoelectronic TiO molecule to better understand the newly observed $E^3\Delta$ state. The electronic configurations giving rise to the observed ground and low-lying electronic states are

$8\sigma^2 3\pi^4 9\sigma^1 1\delta^1$	$X^3\Delta$, $a^1\Delta$	(2)
$8\sigma^2 3\pi^4 9\sigma^2$	$^1\Sigma$	(3)
$8\sigma^2 3\pi^4 9\sigma^1 4\pi^1$	$^3\Pi$, $^1\Pi$	(4)
$8\sigma^2 3\pi^4 1\delta^2$	$^1\Sigma^+$, $^3\Sigma^-$, $^1\Gamma$	(5)
$8\sigma^2 3\pi^4 1\delta^1 4\pi^1$	$^1\Pi$, $^3\Pi$, $^1\Phi$, $^3\Phi$	(6)
$8\sigma^2 3\pi^4 1\delta^1 10\sigma^1$	$^3\Delta$, $^1\Delta$	(7)
$8\sigma^2 3\pi^4 9\sigma^1 10\sigma^1$	$^3\Sigma^+$, $^1\Sigma^+$	(8)

These single electronic configuration explanations are simplistic; however, they lead to a good understanding of the ground and many low-lying electronic states. Table 3 lists the spectroscopic parameters for the low-lying singlet and triplet states observed for TiO and VN. The electronic states arising from the same electronic configuration in TiO and VN are put side by side and are arranged in the order of increasing energy. For simplicity, the triplet states and singlet states are listed

separately. For historical reasons, the letter designations of these states (A, B, C, ..., a, b, c, ...) do not follow their energetic ordering. This situation shows clearly that experimentalists sometimes have difficulties in assigning correct labels to the state found when only partial knowledge of the electronic structure of a molecule is available. The six triplet states expected from the electronic configurations (2), (4)−(8) are all found in TiO. Except for the $D^3\Sigma^-$ state, all of the triplet states are well characterized. For VN, only four triplets state are known; since the newly observed $^3\Delta$ state found in this work is higher in energy than the $D^3\Pi$ state, it is labeled accordingly as the $E^3\Delta$ state. The observed $E^3\Delta-X^3\Delta$ transition is expected to come from the promotion of an electron from the 9σ MO to the 10σ MO. From the MO energy level diagram in Figure 2, it is apparent that the 10σ MO is antibonding in nature. When an electron is removed from a bonding orbital and placed into an antibonding orbital, the bond length of the molecule increases. Increases in bond length by 0.0736 and 0.1271 Å from the ground to the excited $^3\Delta$ state are found respectively for TiO and VN, confirming this expectation. In fact, the $C^3\Delta$ state of TiO and the $E^3\Delta$ state of VN have the longest bond lengths.

Another piece of evidence confirming that the observed $E^3\Delta$ state belongs to the electronic configuration of $1\delta^1 10\sigma^1$ can be found by comparing the spin−orbit separation of the three spin−orbit components. The separation of the highest and lowest spin−orbit components in a degenerate multiplet state is equal to $2A\Lambda S$ when other high-order spin−orbit effects are ignored. For the $X^3\Delta$ and $E^3\Delta$ states of VN, the separations are respectively 302 and 286 cm^{-1}. These values can be correlated to the atomic spin−orbit parameter by applying the microscopic spin−orbit Hamiltonian,[39] $\hat{H}_{so} = \sum_i a_i l_i \cdot s_i$. This is a single-electron operator that can be applied to the Slater determinant wave function. Taking the electronic configuration as $9\sigma^1 1\delta^1$ $X^3\Delta$ and $1\delta^1 10\sigma^1$ $E^3\Delta$, the wave function for the $\Omega = 3$ component is

$$|^3\Delta_3, \sigma^1\delta^1\rangle = |\sigma\alpha\delta^+\alpha|$$

Thus,

$$\langle ^3\Delta_3, \sigma^1\delta^1 | \hat{H}_{so} | {}^3\Delta_3, \sigma^1\delta^1\rangle = \langle \sigma\alpha\delta^+\alpha | \sum_i a_i l_{zi} \cdot s_{zi} | \sigma\alpha\delta^+\alpha\rangle = \alpha_\delta$$

Similarly, for the $\Omega = 1$ component, the $\langle {}^3\Delta_1, \sigma^1\delta^1 | \hat{H}_{so} | {}^3\Delta_1, \sigma^1\delta^1 \rangle = -a_\delta$. Therefore, the spin−orbit separation for a $^3\Delta$ state in a $\sigma^1\delta^1$ electronic configuration is equal to $2a_\delta$. Since the δ MO must be essentially unchanged from its shape in the atom or ion, the a_δ parameter is equivalent to the atomic ζ_{3d} value (151 cm^{-1}).[39] It is easily seen that there is good agreement between the spin−orbit separations of 302 and 286 cm^{-1} for the two $^3\Delta$ states of VN and that of $2a_\delta$ (302 cm^{-1}) for the V^+ ion, which confirms that the electronic configuration of the $X^3\Delta$ and $E^3\Delta$ states does indeed arise from the $\sigma^1\delta^1$ configuration.

A review of the literature indicates that many transient diatomic and small-metal-containing compounds[1,4−6] have been studied using laser-induced fluorescence spectroscopy (LIFS), which is a sensitive technique. The detection of LIF signal relies on the excited molecule dissipating its excess energy through fluorescence. CRLAS is also a sensitive technique, which is suitable for studying transient molecules produced with very low number density or transitions with weak intensity. Saykally and co-workers[31] have demonstrated the application of this technique and have discussed the associated theory in detail. The sensitivity of CRLAS is somewhat comparable to that of LIFS;[31] however, CRLAS has the advantage of not being related to the relaxation pathways of molecules in the excited state. Even though this advantage is not particularly important for many diatomic or small molecules, for medium- to large-size polyatomic molecules such an advantage is significant because the quantum yield for fluorescence is generally very low. The CRLAS instrument used for the present study is very similar to the one used by Saykally and co-workers[31] for studying the spectroscopic properties of gas-phase metal-containing transient species. In our experimental setup, various transient diatomic and polyatomic species can be produced using the laser vaporization/reaction source[31,40,41] that allows vaporized atoms or chemical compounds to react with other reagent chemicals seeded in a carrier gas. The combination of such a laser vaporization/reaction source and CRLAS is a powerful tool for studying the spectroscopy of medium- to large-size transient molecules. We plan to pursue further spectroscopic work on transient polyatmoic species using this instrumental setup.

Acknowledgment. The work described here was supported by a grant from the Research Grants Council of the Hong Kong Special Administrative Region, China (Project No. HKU 7138/99P). We thank Dr. S. J. Xu for his continuous support in this research and the reviewer for suggestions to improve the text.

References and Notes

(1) Huber, K. P.; Herzberg, G. *Constants of Diatomic Molecules*; van Nostrand: New York, 1979.
(2) Bauschlicher, C. W., Jr.; Walch, S. P.; Langhoff, S. R. In *Quantum Chemistry: The Challenge of Transition Metals and Chemistry*; Veillard, A., Ed.; NATO ASI Series C; Reidel: Dordrecht, 1986.
(3) Langhoff, S. R.; Bauschlicher, C. W., Jr. *Annu. Rev. Phys. Chem.* **1988**, *39*, 181.
(4) Merer, A. J. *Annu. Rev. Phys. Chem.* **1989**, *40*, 407.
(5) Hirota, E. *Rep. Prog. Chem., Sect. C: Phys. Chem.* **2000**, *96*, 95.
(6) Bernath, P. F. *Rep. Prog. Chem., Sect. C: Phys. Chem.* **2000**, *96*, 177.
(7) Grunze, M. In *The Chemical Physics of Solid Surfaces and Heterogeneous Catalysis*; King, D. A., Woodruf, D. P., Eds.; Elsevier: New York, 1982; Vol. 4, p 143.
(8) Rao, C. N. R. *Annu. Rev. Phys. Chem.* **1989**, *40*, 291.
(9) Wojuechowsba, M.; Habu, J.; Lomnicki, S.; Stoch, J. *J. Mol. Catal. A: Chem.* **1999**, *141*, 155.
(10) Joyce, R. R.; Hinkle, K. H.; Wallace, L.; Dulick, M.; Lambert, D. L. *Astrophys. J.* **1998**, *116*, 2520.
(11) Nishibayashi, Y.; Iwai, S. Hidai, M. *Science* **1998**, *279*, 540.
(12) Lambert, D. L.; Clegg, R. E. S. *Mol. Not. R., Astron. Soc.* **1980**, *191*, 367.
(13) Lindgren, B.; Olofsson, G. *Astron. Astro. Phys.* 1**980**, *84*, 303.
(14) Cheung, A. S-C.; Hansen, R. C.; Merer, A. J. *J. Mol. Spectrosc.* **1982**, *91*, 165.
(15) Cheung, A. S-C.; Taylor, A. W.; Merer, A. J. *J. Mol. Spectrosc.* **1982**, *92*, 391.
(16) Merer, A. J.; Huang, G.; Cheung, A. S-C.; Taylor, A. W. *J. Mol. Spectrosc.* **1987**, *125*, 465.
(17) Cheung, A. S-C.; Hajigeorgiou, P. G.; Huang, G.; Huang, S.-Z.; Merer, A. J. *J. Mol. Spectrosc.* **1994**, *163*, 443.
(18) Adam, A. G.; Barues, M.; Berno, B.; Bower, R. D.; Merer, A. J. *J. Mol. Spectrosc*. **1995**, *170*, 94.
(19) Ram, R. S.; Bernath, P. F.; Davis, S. P.; Merer, A. J. *J. Mol. Spectrosc*. **2002,** *211*, 279.
(20) Ram, R. S.; Bernath, P. F.; Davis, S. P. *J. Chem. Phys*. **2001**, *114*, 4457.
(21) Ram, R. S.; Bernath, P. F.; Davis, S. P. *J. Chem. Phys*. **2002**, *116*, 7035.
(22) Ran, Q.; Tam, W. S.; Cheung, A. S-C.; Merer, A. J. *J. Mol. Spectrosc*. **2003**, *220*, 87.
(23) Peter, S. L.; Dunn, T. M. *J. Chem. Phys.* **1989**, *90*, 5333.
(24) Simard, B.; Clasoni, C.; Hackett, P. A. *J. Mol. Spectrosc.* **1989**, *136*, 44.
(25) Balfour, W. J.; Merer, A. J.; Nicki, H.; Simard, B.; Hackett, P. A. *J. Chem. Phys*. **1993**, *99*, 3288.
(26) Harrison, J. F. *J. Phys. Chem*. **1996**, *100*, 3513.
(27) Andrews, L.; Bare, W. D.; Chertihin, G. V. *J. Phys. Chem*. **1997**, *101*, 8417.

(28) Steimle, T. C.; Robinson, J. S.; Goodridge, D. *J. Chem. Phys*. **1999**, *110*, 881.
(29) Ram, R. S.; Bernath, P. F.; Davis, S. P. *J. Mol. Spectrosc*. **2001**, *210*, 110.
(30) Ram, R. S.; Bernath, P. F.; Davis, S. P. *J. Mol. Spectrosc*. **2002**, *215*, 163.
(31) Scherer, J. J.; Paul, J. B.; O'Keefe, A.; Saykally, R. J. *Chem. Rev*. **1997**, *97*, 25.
(32) Ma, T.; Leung, J. W-H.; Cheung, A. S-C. *Chem. Phys. Lett*. **2004**, *385*, 259.
(33) Edlen, B. *Metrologia* **1966**, *2*, 71.
(34) Brown, J. M.; Kopp, I.; Malmberg, C.; Rydh, B. *Phys. Ser*. **1978**, *17*, 55.
(35) Brown, J. M.; Cheung, A. S-C.; Merer, A. J. *J. Mol. Spectrosc*. **1987**, *124*, 464.
(36) Bauschlicher, C. W.; Bagus, P. S.; Nelin, C. J. *Chem. Phys. Lett.* **1983**, *101*, 229.
(37) Sennesal, J. M.; Schamps, J. *Chem. Phys*. **1987**, *114*, 37.
(38) Langhoff, S. R. *Astrophys. J.* **1977**, *481*, 1007.
(39) Lefebvre-Brion, H.; Field, R. W. *Perturbations in the Spectra of Diatomic Molecules*; Academic Press: New York, 1986.
(40) Simard, B.; Mitchell, S. A.; Humphires, M. R.; Hackett, P. A. *J. Mol. Spectrosc*. **1988**, *129*, 189.
(41) Kappes, M. M. *Chem. Rev*. **1988**, *88*, 369.